Applied Energy 195 (2017) 646–658

Contents lists available at ScienceDirect

Applied Energy

journal homepage: www.elsevier.com/locate/apenergy

Performance analysis of a supercritical water-cooled nuclear reactor integrated with a combined cycle, a Cu-Cl thermochemical cycle and a hydrogen compression system

Maan Al-Zareer *, Ibrahim Dincer, Marc A. Rosen

Clean Energy Research Laboratory, Faculty of Engineering and Applied Science, University of Ontario Institute of Technology, 2000 Simcoe Street North, Oshawa, Ontario L1H 7K4, Canada

HIGHLIGHTS

- Integrated nuclear-based hydrogen production plant is proposed.
- Performance of the integrated system is measured through thermodynamic analysis.
- New design for the Cu-Cl cycle is proposed for integrating it with SCWR.

GRAPHICAL ABSTRACT

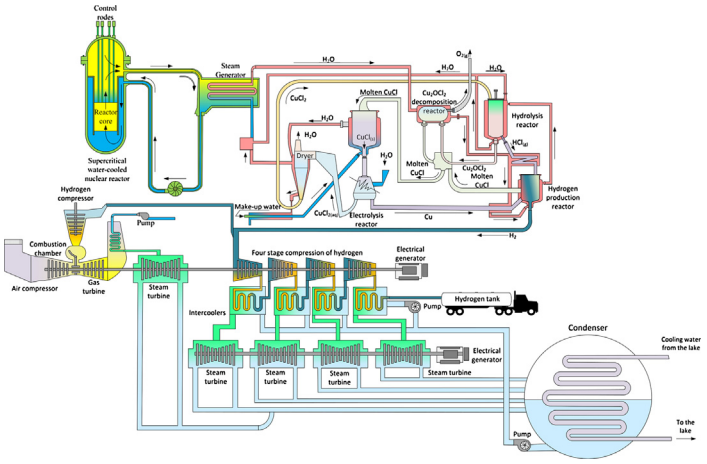

ARTICLE INFO

Article history:
Received 1 November 2016
Received in revised form 1 February 2017
Accepted 10 March 2017
Available online 27 March 2017

Keywords:
Hydrogen production
Energy
Exergy
Efficiency
Nuclear power
Copper-chlorine cycle

ABSTRACT

A novel integration is proposed and analyzed of a thermochemical water decomposition cycle with a supercritical water-cooled nuclear reactor, a combined cycle, and a hydrogen compression system. The supercritical water-cooled reactor in the integrated system has been investigated extensively in Canada. The integrated system uses a compression system to compress the product hydrogen. The hydrogen is produced via a hybrid thermochemical and electrical water decomposition cycle that utilizes the chemical couple of copper and chlorine. The integrated system is modeled and simulated on Aspen Plus, except for the steam circuit, which is simulated on Aspen Hysys. The hydrogen production rate from the proposed system is 3.56 kg/s. Both energy and exergy analyses are performed of the integrated system, and its overall energy and exergy efficiencies are, in this regard, found to be 16.9% and 27.8%, respectively.

1. Introduction

Hydrogen is abundant in nature; it accounts for 75% (mass basis) and 90% (by number of atoms) of the total matter in the

* Corresponding author.
E-mail addresses: maan.al-zareer@uoit.ca (M. Al-Zareer), ibrahim.dincer@uoit.ca (I. Dincer), marc.rosen@uoit.ca (M.A. Rosen).

http://dx.doi.org/10.1016/j.apenergy.2017.03.046
0306-2619/

Nomenclature

$\dot{E}x$	exergy rate (kW)
ex	specific exergy (kJ/kg)
LHV	lower heating value (kJ/kg)
h	specific enthalpy (kJ/kg)
h_f	heat of formation
$\dot{m}$	mass flow rate (kg/s)
P	pressure (kPa)
$\dot{Q}$	heat rate (kW)
T	temperature (°C)
$\dot{W}$	work rate (kW)

Greek letters

η	energy efficiency
ψ	exergy efficiency

Subscripts

bs	boundary where heat transfer occurs
c	compressor
Cu-Cl	copper-chlorine
d	destruction
e	electrical
gen	generation
GT	gas turbine
H_2	hydrogen
HCS	hydrogen compression system
is	isentropic
in	input (flowing into the system boundary)
net	net result
ov	overall
out	output (flowing out of the system boundary)
o	reference environment conditions
p	pump
$\dot{Q}$	heat flow rate
RC	Rankine cycle
ST	steam turbine
SCC	supporting combined cycle

Superscripts

HP	hydrogen at high pressure (700 bar)
LP	hydrogen at low pressure

Acronyms

Cu-Cl	copper-chlorine cycle
ER	electrolysis reactor
HCS	hydrogen compression system
RC	Rankine cycle
SC	steam circuit
SCC	supporting combined cycle
SCWR	supercritical water-cooled nuclear reactor

Aspen Plus terms (italic terms)

Rstoic	Aspen Plus reactor model that carries out the reaction based on the stoichiometric balanced chemical reaction equation with a specified reactants conversion percentage
Cisolid	for homogeneous solids that have a defined molecular weight, with the option of entering the particle size distribution
RGibbs	Aspen Plus reactor model that carries out the reaction based on Gibbs free energy minimization approach
Mixed	material stream option in Aspen Plus modeling

universe [1]. On earth, an abundant amount of hydrogen exists connected to an oxygen atom in the form of water (H_2O) [2]. The chemical bond between a hydrogen atom and an oxygen atom in water requires 460 kJ/mol of energy to break [3,4]. Hydrogen in the form of H_2 has the highest energy to mass density of any substance. But hydrogen is not readily available in nature in large amounts in the form of H_2. Hydrogen can serve as an energy storage medium and as a clean energy carrier. Many technologies are available for producing hydrogen from water, such as water electrolysis, thermal water decomposition, thermochemical water decomposition, and thermochemical and electrical water decomposition. Water decomposition is a potentially attractive method for hydrogen production.

Energy demands of the world are continuously rising, with recent reports from the International Energy Agency expecting an increase of 50% from 2016 to 2030 [5]. Energy demands vary yearly, monthly and daily, so it if is challenging for power plants intended to meet the energy demands exactly. The benefits of steady-state conditions are lost, and the efficiency of the power plant is reduced. Another option for maintaining a constant operational rate for a power plant and at the same time not losing energy is by using energy storage. One energy storage option is hydrogen. Hydrogen has one of the highest energy to mass densities of any substance. Also, hydrogen energy can be produced from water using various methods using heat, electricity, and chemical fuels. When produced from water without hydrocarbon fuels, hydrogen is a clean fuel in terms of carbon-based emission, which provides an advantage as an energy storage and energy carrier.

Most hydrogen is produced today from fossil fuels, mainly via steam reforming of natural gas. There are also other processes for obtaining hydrogen from fossil fuels such as coal gasification, and catalytic combustion and partial oxidation of other hydrocarbons [6]. Other methods produce hydrogen from renewable resources, such as biomass gasification [7] and solar hydrogen production [8]. Hydrogen production from fossil fuels is not environmentally benign, since it yields carbon-based emissions, which are greenhouse gases and one of the main contributors to global warming. Hydrogen production from non-carbon based fuels avoids carbon-based emissions. A large percentage of hydrogen on earth is in the form of water, so water decomposition to produce hydrogen using a non-carbon emitting process can be advantageous for reducing carbon emissions.

Thermochemical and electrical water decomposition powered thermally by nuclear reactors is a promising technology for producing hydrogen without carbon-emissions. The thermochemical and electrical water decomposition processes requires heat at lower temperatures than those required when directly decomposing water thermally. The thermochemical and electrical water decomposition cycle that is based on the chemical couple copper and chlorine (Cu-Cl cycle) has one of the lowest temperature requirements for thermochemical water decomposition. Nonetheless, the Cu-Cl cycle requires temperatures higher than available from currently operating nuclear reactors [9]. The relatively low steam temperature of current nuclear reactors is one of the main reasons for their relatively low efficiencies. New nuclear reactors concepts are being introduced that involve higher steam temperatures. One promising concept is the supercritical water-cooled nuclear reactor (SCWR). The SCWR produces steam at an outlet temperature of 625 °C [10]. One reason for coupling a Cu-Cl cycle with a SCWR rather than with a supercritical Rankine cycle where

the produced energy is required in the H_2 form relates to efficiency, in that the efficiency for such a Cu-Cl cycle was reported by Orhan, Dincer and Rosen [11–13] and Ratlamwala and Dincer [14] to range between 40.1% and 44.8%. However, the efficiency of a supercritical Rankine cycle with single reheat simulated by Al-Zareer et al. [15] was 36.2% and to produce hydrogen it has to be coupled with another system to convert electrical energy to hydrogen. This means that a supercritical Rankine cycle with a single reheat integrated with electrical energy to hydrogen conversion system will have an overall energy efficiency less than 36.2%. Thus, the Cu-Cl cycle has a much higher energy efficiency of nearly 10% more when the end product that is required in the form of H_2.

Relatively few thermodynamic studies of the Cu-Cl cycle have been reported, and there are few studies on designs for providing the heat to the Cu-Cl cycle reactors (in a steam circuit) when the Cu-Cl cycle is integrated with a steam producing system (such as a SCWR), i.e., the flow behavior of the steam through the reactors of the Cu-Cl cycle has not been thoroughly investigated. Some researchers propose a heat exchanger network for transferring the required heat between the steam exiting the nuclear reactor and the Cu-Cl cycle chemical reactors, such as Ozbilen et al. [16]. However, in [16] a specific design for the steam circuit is not specified clearly. The aim of this paper is to integrate the SCWR with the Cu-Cl cycle using a defined steam circuit (SC), which is lacking in the literature, a hydrogen compression system (HCS) and a supporting combined cycle (SCC). The purpose of proposing an SC in this paper is highly motivated by the fact that only simulating the water electro-thermo-chemical decomposition process is insufficient to provide comprehensive understanding. Rather, the process of delivering and receiving the thermal energy to and from the components of the Cu-Cl cycle is also important, and providing this understanding is the objective of this study. This paper describes and demonstrates the importance of considering an SC, when steam is the heat transfer fluid used to deliver thermal energy to the reactors. Then the integrated system is simulated using Aspen Plus software, and a thermodynamic analysis is performed on the proposed integrated system. The Cu-Cl cycle with a SC is compared using simulation with other cycles without a SC (based on energy requirements). The energy and exergy efficiencies and the hydrogen production flow rate are reported for each case of the Cu-Cl cycle. The SC is simulated in Aspen Hysys.

2. System description

The proposed integrated system for producing compressed hydrogen is shown in Fig. 1, which presents a new design concept for the five reactors of the Cu-Cl cycle and how the SC is organized. The thermal energy driving the integrated system comes from the SCWR though the steam generator as shown in Fig. 1. The supercritical pump is used only to restore pressure losses through the steam generator. The parameters and the outlet thermal energy of the SCWR are given in Table 1 [10]. Since the maximum required steam temperature by the Cu-Cl cycle is 530 °C and the SCWR can provide temperature up to 625 °C, the systems are complementary. Since the Cu-Cl cycle requires steam at atmospheric pressure the supercritical water of the nuclear reactor continues circulating in a closed circuit, and the steam conveyed to the Cu-Cl cycle is on a different circuit. The current design of the Cu-Cl cycle is described next.

The proposed design of the Cu-Cl cycle is shown in Figs. 1, 2a, and 3 and the main chemical reactions that take place in the cycle

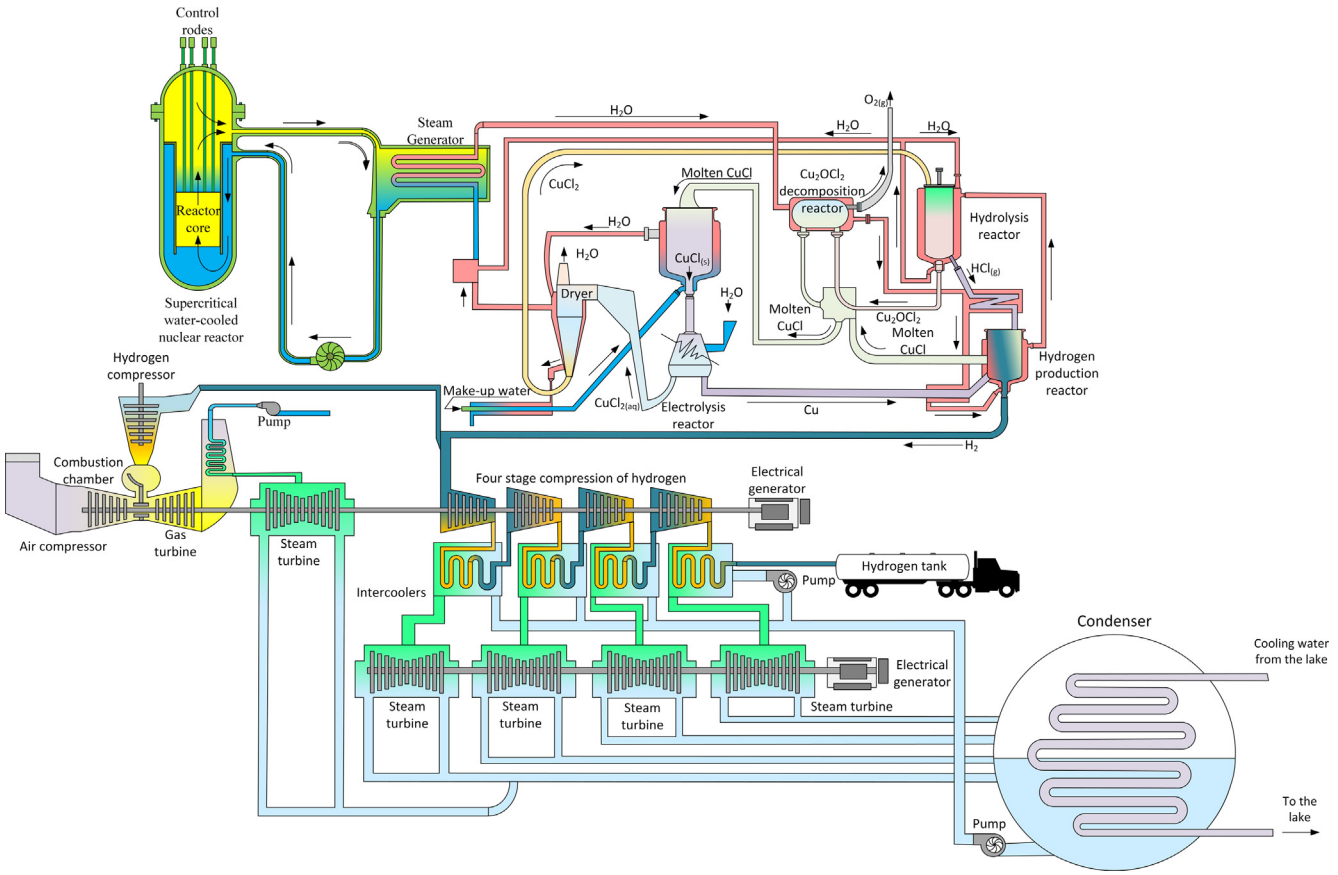

Fig. 1. Proposed integrated system that integrates the SCWR concept with a new Cu-Cl cycle design with a steam circuit, supporting combined cycle, and a hydrogen compression system.

Table 1
Main parameters in the proposed integrated system, consisting of SCWR, Cu-Cl cycle, supporting combined cycle, and hydrogen compression system.

Component	Parameter	Value	Unit	Ref.
SCWR	Temperature of steam exiting reactor	625	°C	[10,19]
	Temperature of water returning to reactor	350	°C	[10,19]
	Operating pressure of nuclear reactor	25	MPa	[10,19]
	Thermal energy output	2540	MW	[10,19]
	Supercritical steam mass flow rate	1320	kg/s	[10,19]
	T_{max} cladding	850	°C	[10,19]
Cu-Cl cycle	Table 2 contains data for main cycle reactions and Tables 3a and 3b for thermochemical properties of the main Cu-Cl cycle materials that appear in the solid phase in the cycle			
Hydrogen compression system	Hydrogen final pressure	700	bar	[20,21]
	Number of compression stages	4	stages	
	Pressure ratio of each stage except final stage	5		
	Rankine cycle connected to intercoolers			
	RC1 operating pressure	20	bar	
	RC2 operating pressure	20	bar	
	RC3 operating pressure	20	bar	
	RC4 operating pressure	30	bar	
	$\eta_{is,C}$	0.72		[22]
	$\eta_{is,ST}$	0.72		[22]
Supporting combined cycle	Combustion chamber pressure	36	bar	
	Air compressor pressure ratio	36		
	Hydrogen compressor pressure ratio	36		
	Rankine cycle operating pressure	200	bar	
	$\eta_{is,GT}$	0.72		[22]
	$\eta_{is,ST}$	0.72		[22]
	$\eta_{is,C}$	0.72		[22]

are listed in Table 2 and graphically presented in Fig. 2b. Fig. 3 shows the proposed steam circuit design for providing the Cu-Cl cycle with the required heat and steam and for recovering part of the heat released by the Cu-Cl cycle itself. Fig. 3 is also labeled with the names of the reactors in Fig. 2a. The steam jackets around the reactors are the method of delivering the thermal energy to these reactors and the steam is the heat transfer fluid. Water at environment conditions is first heated (in heat exchanger E-110) by the steam exiting the steam jacket of the dryer (B12). The generated steam (at 120 °C in Fig. 3) is superheated with the heat recovered from cooling the solid CuCl in heat exchanger B11 to 140 °C. Steam exiting the heat exchanger (B11) enters the steam jacket (E-104) of the CuCl phase change reactors (B8 and B28) and exits at a high temperature of 434 °C. Then it enters the steam jacket (E-108) of the dryer and cools to 265 °C. The steam exiting the steam jacket of the dryer is split (through the splitter TEE-101) to a ratio of 1–60 (mole basis). The main portion of the split steam is sent back to the heat exchanger (E-101) and exits at 83.1 °C and is then rejected in the lake. The smaller portion is mixed steam (mixer MIX-100) with the excess steam exiting the hydrolysis reactor and with the other steam used to circulate in a closed cycle for heat exchange purposes.

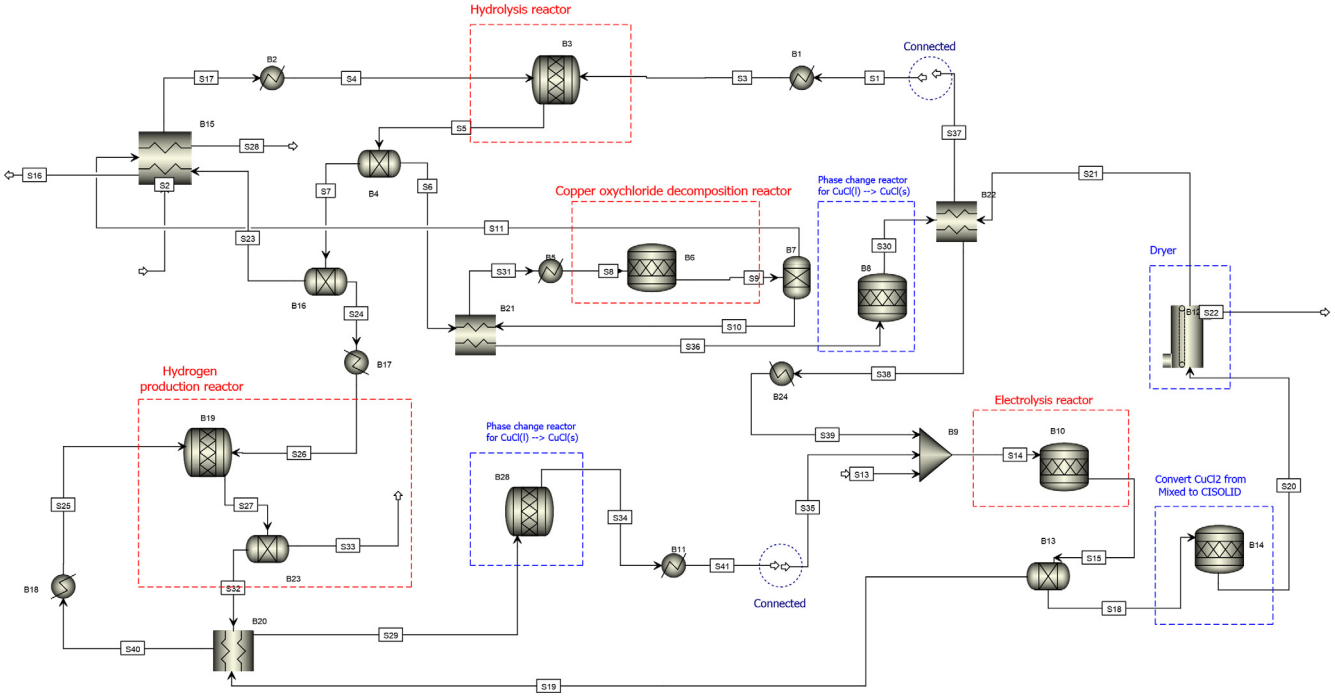

Fig. 2a. Aspen Plus flow sheet of the Cu-Cl cycle in the proposed integrated system.

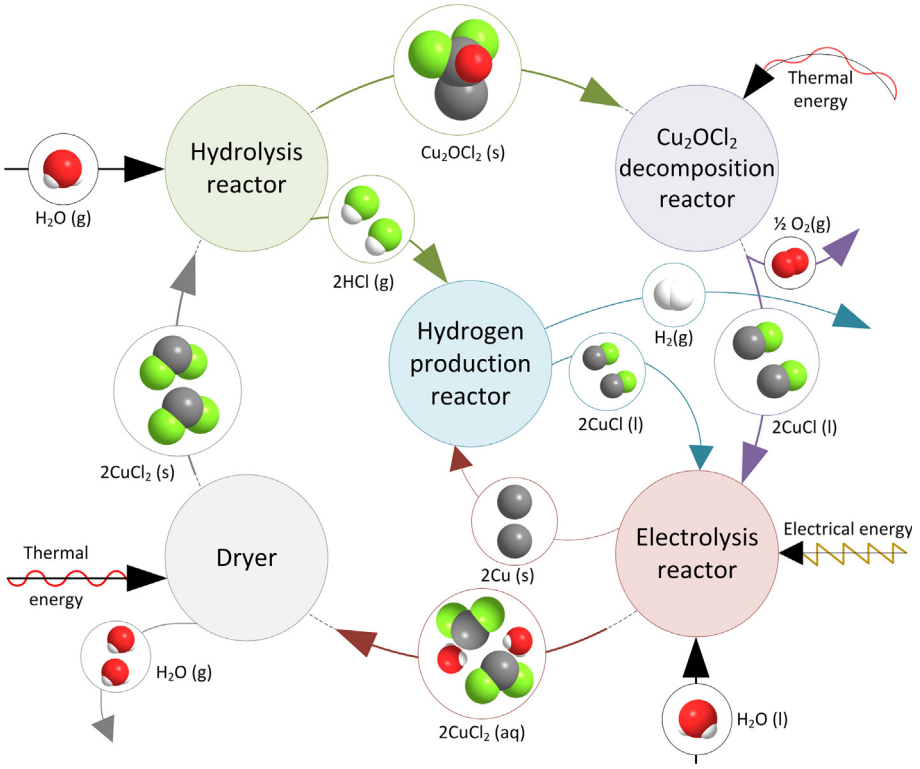

Fig. 2b. Main interactions that occur in the steps of the five-step Cu-Cl cycle for thermochemical water decomposition in the integrated system.

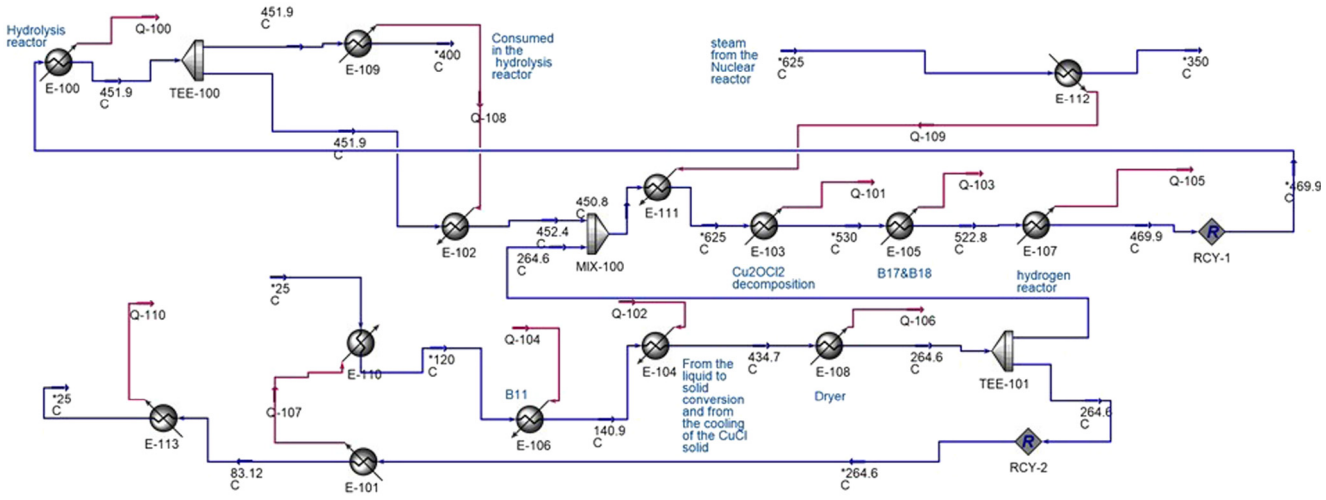

Fig. 3. Aspen Hysys flow sheet of the proposed steam circuit for the Cu-Cl cycle in the integrated system.

Table 2
Cu-Cl cycle reactions based on the five-step cycle and corresponding reactions and operating conditions [13,23].

Step	Reactor name	Chemical reaction	Temperature range (°C)
1	Hydrolysis reactor	$H_2O(g) + 2CuCl_2(s) \rightarrow Cu_2OCl_2(s) + 2HCl(g)$	375–400
2	Cu_2OCl_2 decomposition reactor	$Cu_2OCl_2(s) \rightarrow \frac{1}{2}O_2(g) + 2CuCl(l)$	500–530
3	Hydrogen production reactor	$2Cu(s) + 2HCl(g) \rightarrow 2CuCl(l) + H_2(g)$	430–475
4	Electrolysis reactor (requires 63 kJ/mol of electricity) [23]	$4CuCl(aq) \rightarrow 2Cu(s) + 2CuCl_2(aq)$	30–80
5	Dryer	$CuCl_2(aq) \rightarrow CuCl_2(s)$	>100

Then the mixed product enters the heat exchanger that exchanges heat with the supercritical steam exiting the nuclear reactor. The resulting superheated steam enters the steam jacket of the Cu_2OCl_2 decomposition reactor (B6) and the preheater (B5) and maintains the reactor temperature at 530 °C (see Table 2). Then the steam exiting the steam jacket of B6 heats the HCl and solid cop-

Table 3a
Materials in copper-chlorine thermochemical water decomposition cycle and their properties and correlations used in the developed copper-chlorine cycle Aspen Plus simulation model, for temperature range of 298–675 K at 1 atm.

Material	Copper oxychloride (Cu_2OCl_2, melanothallite)	
parameter	Value or correlation[a]	Ref.
Molecule formation	$\Delta_f H^o = -384.65 \pm 2.5$ kJ/mol $\Delta_f S^o = 154.352$ J/mol · K $\Delta_f G^o = -369.7$ kJ/mol $\log k_f = 64.75$ $ex_{ch} = 21.08$ kJ/mol $c_p^o = 116.77$ kJ/kmol · K $T_o = 298.15$ K and $P_o = 1$ atm	[23,24]
c_p (kJ/kmol · K)	$a + bT + cT^2 + dT^3$ $a = 53.7166572;\ b = 0.334033497;\ c = -5.22127940 \times 10^{-4};\ d = 2.99950910 \times 10^{-7}$	[23]
s (J/mol · K)	$a + b\ln(T) + cT + dT^2 + eT^3$ $a = 154.352;\ b = 53.7166572:\ c = 0.334033497;\ d = -0.2610639700 \times 10^{-3}$	[23]
ex (J/mol)	$a + bT + cT^2 + dT^3 + eT^4 + f\ln(T)$ $a = 0.358948789 \times 10^5;\ b = -45.87542993;\ c = 0.2448529712;\ d = -0.2038527680 \times 10^{-3}, e = 1.3589 \times 10^5,\ f = -16015.62134$	[23]
Material	Cupric oxide (CuO, tenorite)	
Parameter	Value or correlation[a]	Ref.
Molecule formation	$\Delta_f H^o = -156 \pm 2.1$ kJ/mol $\Delta_f S^o = 42.59 \pm 0.4$ J/mol · K $\Delta_f G^o = -128.292$ kJ/mol $\log k_f = 22.48$ $ex_{ch} = 6.268$ kJ/mol $c_p^o = 42.18$ kJ/kmol · K $T_o = 298.15$ K and $P_o = 1$ atm	[23,25]
c_p (kJ/kmol · K)	$a + bT + cT^2 + dT^3 + e$ $T^{-2};\ a = 52.465081,\ b = -0.0145802613,\ c = 4.51372247 \times 10^{-5},\ d = -2.91900324 \times 10^{-8};\ e = -816,025.22$ with error$^{+0.05}_{-0.1}$ kJ/kmol · K	[23]
s (J/mol · K)	$a + bT + cT^2 + dT^3 + e\ln(T) + fT^{-2}$ $a = -258.3259972;\ b = -0.0145802613;\ c = 2.256861235 \times 10^{-5}:\ d = -9.730010800 \times 10^{-9};\ e = 52.465081;\ f = 4.0801261 \times 10^5$	[23]
ex (J/mol)	$a + bT + cT^2 + dT^3 + eT^4 + fT^{-1} + gT^{-2} + h\ln(T)$ $a = 77,913.62262;\ b = 56.81218591;\ c = -0.01401896242;\ d = 0.1794674429 \times 10^{-4};\ e = -7.297508100 \times 10^{-9};\ f = 8.160252200 \times 10$	[23]

[a] If the correlation model (i.e. $aT+bT^2\ldots$) is not available in Aspen Plus, an excel table of T vs "variable" is produced and data is entered in Aspen Plus.

per (in heat exchangers B17 and B18 in Fig. 2a and E-105 in Fig. 3) to the operating temperature of the hydrogen reactor (B19), and then enters the hydrogen reactor steam jacket (E-107). The steam exiting E-107 is sent to the hydrolysis reactor (B3) steam jacket (E-100) to provide the heat required by the hydrolysis reactor. The steam exiting E-100 is split in splitter TEE-100; part enters the hydrolysis reactor and part is consumed while the rest is sent to the MIX-100 to complete the upper steam circuit cycle. Since the hydrolysis reactor consumes steam, which is one of the reactants in the hydrolysis reaction, then part of the steam that delivered parts of its thermal energy to the hydrolysis reactor is sent to the reactor by a two-way valve. The final two reactors in the Cu-Cl cycle Aspen Plus model that are not present in the steam circuit model are the electrolysis reactor (B10) and the reactor (B14). Reactors B10 and B14 are not considered in the steam circuit model because they do not require or produce any heat. Reactor B14 is required to convert the solid form of $CuCl_2$ in its aqueous solution from *mixed* to *cisolid* solid type before feeding the aqueous solution to the dryer (B12).

Note that the only material defined in the steam circuit is water, and the heat rates (into the water or out of the water) are determined from the Aspen Plus model of the Cu-Cl cycle. Not all of the heat released while cooling stream S34 is transferred to the water due to temperature limitations. The temperature limitations refer to the difference between the temperature of the steam and the temperature of the CuCl. The heat transfer between the solidifying and then cooling CuCl and the steam depends on the temperature difference between the two. When the temperature difference reaches a small value no more heat is absorbed by the steam, and then other cooling means will be used to reduce the temperature of the solid CuCl to the required temperature of the electrolysis reactor. The HCS Aspen Plus flowsheet is shown in Fig. 4, and the Aspen Plus flowsheet of the SCC is provided in Fig. 5. The HCS contains four hydrogen compressors, four intercoolers, and four bottoming Rankine cycles. The first three hydrogen compressors have a compression ratio of 5, and the fourth hydrogen compressor has a discharge pressure of 700 bar. The intercooler generates steam for the bottoming Rankine cycles; which reduce the required power for the hydrogen compression process through recovering heat from the intercoolers. The SCC takes part of the produced hydrogen and generates work to fulfill the integrated system power requirements. The SCC consist of two compressors (C5 and C6) as shown in Fig. 5. C5 compresses hydrogen and the compressor C6 the required air for the combustion process. Both compressors have a compression ratio of 36. The molar ratio of air to hydrogen is 9.18. The combustion chamber operating pressure is 36 atm. The combustion chamber is modeled using an *RGibbs* reactor model in Aspen Plus, in which the reaction among the reactants occurs based on the Gibbs free energy minimization approach. The maximum operating pressure is 200 bar in the Rankine cycle part of the combined cycle.

In the next section, the thermodynamics analysis of the proposed integrated system is presented.

3. Analysis

The main assumptions made during the development of the proposed integrated system of the SCWR, the Cu-Cl cycle, the HCS, and the SCC are listed as follows:

Table 3b
Materials in copper-chlorine thermochemical water decomposition cycle and their properties and correlations used in the developed copper-chlorine cycle Aspen Plus simulation model, for temperature range of 298–675 K and at 1 atm.

Material	Cupric chloride ($CuCl_2$, tolbachite)		
Parameter	Value or correlation[a]		Ref.
Melting point	498 °C		[26]
Normal boiling point	993 °C		[26]
Decomposition temperature to Cu_2Cl_2	993 °C		[26]
Molecule formation	$\Delta_f H^o = -218.0$ kJ/mol $\Delta_f S^o = 108.07$ J/mol · K $\Delta_f G^o = -173.826$ kJ/mol $\log k_f = 30.453$ $ex_{ch} = 82.474$ kJ/mol $c_p^o = 71.88$ kJ/kmol · K $T_o = 298.15$ K and $P_o = 1$ atm		[23,27]
c_p (kJ/kmol · K)	T = 298–675 K, crystal I	$a + bT + cT^2 + dT^3 + eT^4 + fT^5$, $a = -16.3596145$; $b = 0.750699416$, $c = -2.56737967 \times 10^{-3}$; $d = 4.62107127 \times 10^{-6}$; $e = -4.34415987 \times 10^{-9}$; $f = 1.57231698 \times 10^{-12}$	[23]
	675–871 K, crystal II	82.4	
	For the liquid Phase, Aspen Plus library has the required data		
s (J/mol · K)	T = 298–675 K, crystal I	$a + bT + cT^2 + dT^3 + eT^4 + fT^5 + g\ln(T)$ $a = 58.38957705$, $b = 0.750699416$; $c = -1.283689835 \times 10^{-3}$; $d = 1.54035709 \times 10^{-6}$; $e = -1.061039968 \times 10^{-9}$; $f = 3.14463396 \times 10^{-13}$; $g = -16.3596145$	[23]
	T = 675–871 K, crystal II	$172.2201546 + 82.4\ln(T/675)$	
	For the liquid Phase, Aspen Plus library has the required data		
ex(J/mol)	$a + bT + cT^2 + d\ln(T)$		[23]
	T = 298–675 K	$a = 1.850096 \times 10^5$; $b = 68.091341$; $c = 0.69649 \times 10^{-2}$; $d = -21,667.1954$	
	T = 675–871 K	$a = 1.978071674$; $b = 82.4$; $c = 1.835569 \times 10^{-9}$; $d = -24,567.55627$	
	T = 871–1130.75 K	$a = 2.278675157$; $b = 100$; $c = -6.751777 \times 10^{-9}$; $d = -29815.02$	

Material	Cuprous chloride (CuCl, nantokite)					
Parameter	Value or correlation[a]					Ref.
Melting point	436 °C					[28]
Normal boiling point	1221.85 °C					[25]
Vapor pressure	Vapor pressure at the triple point is 10.19 Pa					[26,27]
	T (°C)	459	543	675	914	1477
	P (kPa)	0.010	0.100	1.000	10.00	100.0
Molecule formation	$\Delta_f H^o = -136.816$ kJ/mol $\Delta_f S^o = 87.446$ J/mol · K $\Delta_f G^o = -199.44$ kJ/mol $\log k_f = 21.02$ $ex_{ch} = 75.0$ kJ/mol $c_p^o = 53.34$ kJ/kmol · K $T_o = 298.15$ K and $P_o = 1$ atm					[23,25]
c_p (kJ/kmol · K)	T = 298–683 K	$a + bT + cT^{-2}$ $a = 51.087$; $b = 17.656 \times 10^{-3}$; $c = 268 \times 10^3$				[28]
s (J/mol · K)	T = 298–683 K	$a + b\ln(T) + cT + dT^{-2}$ $a = -210.3986829$, $b = 51.087$; $c = 0.017656$; $d = 1.34 \times 10^5$				[23]
ex (J/mol)	T = 298–683 K	$a + bT + cT^2 + dT^{-1} + eT^{-2} + f\ln(T)$ $a = 191,327.176$; $b = 45.823$; $c = 0.008828$; $d = 268,000$; $e = 3.9952 \times 10^7$; $f = -15,231.589$				[23]

[a] If the correlation model (i.e. $aT+bT^2\ldots$) is not available in Aspen Plus, an excel table of T vs "variable" is produced and data is entered in Aspen Plus.

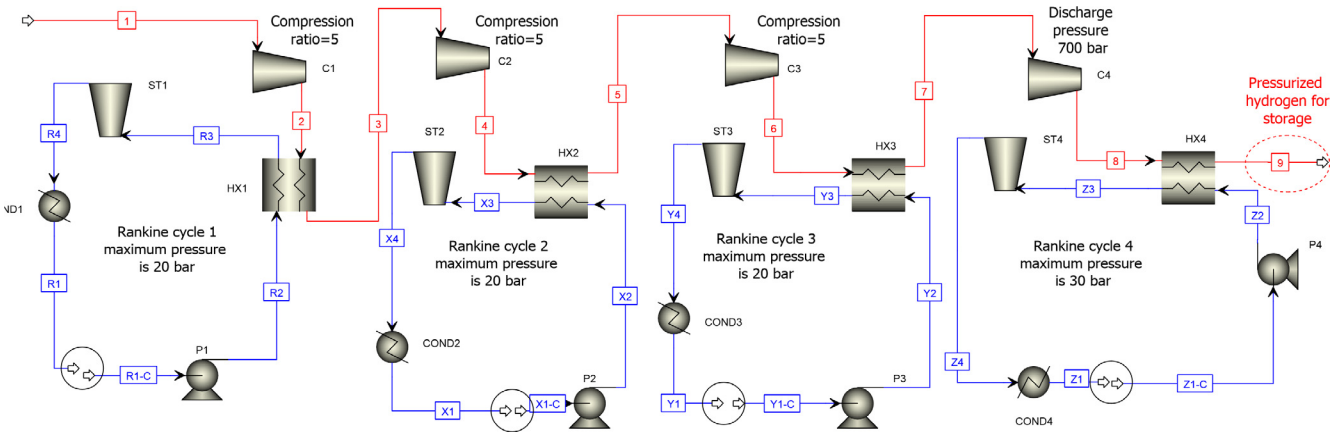

Fig. 4. Hydrogen compression system (HCS) Aspen Plus simulation flowsheet.

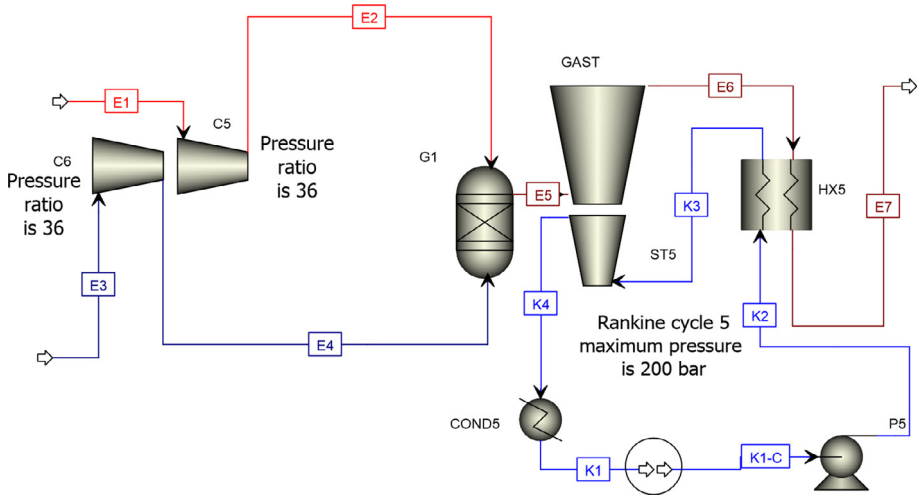

Fig. 5. Supporting combined cycle (SCC) Aspen Plus simulation flowsheet.

- The steady state conditions apply to all components of the integrated system.
- The energy changes associated with gravitational and kinetic energies are not taken into consideration.
- The efficiency of the electrical generator ranges from 35% of small size generators to over 97% for large generators and the selected efficiency is 95% which is closer to the large generators efficiencies since the proposed in this paper is large scale power and hydrogen plant.
- The heat losses for heat exchangers are neglected.
- Due to the high average capacity factor of Canadian nuclear reactors, the reactors are taken to operate at steady state conditions [10,17].
- The pressure losses are negligible in all heat exchangers.
- The compressors and turbines operate under adiabatic conditions.

In the analysis, the reference environment temperature and pressure for exergy calculations are specified to be 25 °C and 1 atm, respectively.

An important step in building the Aspen Plus model and successfully running the simulation is selecting the appropriate property method. The properties chosen for the construction of the models are as follows:

Aspen Plus selected property methods:

- For H_2O: *Steamnbs* for the temperature range of 273 K–2000 K at a maximum pressure of over 10,000 bar.
- For the remaining materials: Rk-Soave.

Aspen Hysys selected property methods:

- For H_2O: NBS steam tables.

The analysis utilizes the general rate balance equations of mass, energy, and exergy for a steady state flow process, which are as follows [18]:

$$\sum \dot{m}_{in} - \sum \dot{m}_{out} = 0 \tag{1}$$

$$\dot{Q}_{in} - \dot{Q}_{out} + \dot{W}_{in} - \dot{W}_{out} = \sum_{out} \dot{m}(h_{P\&T} - h_{T_o\&P_o} + h_f) - \sum_{in} \dot{m}(h_{P\&T} - h_{T_o\&P_o} + h_f) \tag{2}$$

$$\dot{E}x_{\dot{Q}_{in}} - \dot{E}x_{\dot{Q}_{out}} + \dot{E}x_{\dot{W}_{in}} - \dot{E}x_{\dot{W}_{out}} = \sum_{out} \dot{m}_{out} ex_{out} - \sum_{in} \dot{m}_{in} ex_{in} + \dot{E}x_d \tag{3}$$

Here, $\dot{m}$ is the mass flow per unit time, $\dot{W}$ is the work per unit time (power), h is the specific enthalpy of a flowing stream, h_f is the heat of formation of each chemical molecule (element or compound),

ex is the specific exergy of a flowing stream, and $\dot{E}x_d$ is the exergy destruction per unit time. Also, the subscript in denotes input and out output, while $\dot{E}x_{\dot{Q}}$ is the exergy flow per unit time that is associated with heat transfer rate $\dot{Q}$, expressible as

$$\dot{E}x_{\dot{Q}} = \left(1 - \frac{T_o}{T_{bs}}\right)\dot{Q} \tag{4}$$

The balance equations can be applied to the integrated system as a whole, and to its subsystems and components.

Efficiencies for the integrated system and its subsystems and components can be expressed as follows [18]:

$$\eta = \frac{\text{Energy in product outputs}}{\text{Energy in inputs}} \tag{5}$$

$$\psi = \frac{\text{Exergy in product outputs}}{\text{Exergy in inputs}} \tag{6}$$

where η is the energy efficiency and ψ the exergy efficiency.

The energy and exergy efficiencies of the subsystems as well as the overall integrated system are provided. The integrated system is divided into the following subsystems: SCWR, Cu-Cl cycle, HCS, and SCC. The SCWR efficiencies are not calculated since the nuclear reaction is not modeled; rather its outputs are adopted from the work of Bushby et al. [19] and presented in Table 1. While determining the energy and exergy efficiencies and the hydrogen production rate, two cases are taken into account. The two cases consider the effect of the design of the steam circuit on the performance of the Cu-Cl cycle and on the integrated system as a whole.

The energy and exergy efficiencies respectively of the Cu-Cl cycle are as follows:

$$\eta_{Cu-Cl} = \frac{\dot{m}_{H_2}(LHV_{H_2})}{\dot{Q}_{net,in} + \dot{W}_e} \tag{7}$$

$$\psi_{Cu-Cl} = \frac{\dot{m}_{H_2} ex_{H_2}}{\dot{E}x_{\dot{Q}_{net,in}} + \dot{W}_e} \tag{8}$$

where $\dot{Q}_{net,in}$ is for the first case (not considering the steam circuit design) the summation of all heat rate interactions in the Cu-Cl cycle, and for the second case (considering a novel steam circuit design) is the heat rate that the cycle absorbs from the supercritical steam from the SCWR. Also, $\dot{E}x_{\dot{Q}_{net,in}}$ is the exergy rate associated with $\dot{Q}_{net,in}$.

The energy and exergy efficiencies respectively of the HCS are as follows:

$$\eta_{HCS} = \frac{\left(\dot{m}_{H_2}^{HP} h_{H_2}^{HP} - \dot{m}_{H_2}^{LP} h_{H_2}^{LP}\right)}{\dot{W}_C - \dot{W}_{ST} + \dot{W}_p} \tag{9}$$

$$\psi_{HCS} = \frac{\left(\dot{m}_{H_2}^{HP} ex_{H_2}^{HP} - \dot{m}_{H_2}^{LP} ex_{H_2}^{LP}\right)}{\dot{W}_C - \dot{W}_{ST} + \dot{W}_p} \tag{10}$$

where the superscripts HP and LP denote high-pressure hydrogen and low-pressure hydrogen, respectively, while the subscripts C, ST, and P refer to compressors, steam turbines, and pumps respectively.

The energy and exergy efficiencies respectively of the SCC are written as follows:

$$\eta_{SCC} = \frac{\dot{W}_{net,out}}{\dot{m}_{H_2} LHV_{H_2}} \tag{11}$$

$$\psi_{SCC} = \frac{\dot{W}_{net,out}}{\dot{m}_{H_2} ex_{H_2}} \tag{12}$$

Table 4
Simulation results for proposed integrated system for hydrogen production for the two cases.

Parameter	Unit	Case 1	Case 2
Case description		Including proposed steam circuit design	Excluding proposed steam circuit design
SCC energy efficiency (η_{SCC})	%	39.7	39.7
SCC energy efficiency (ψ_{SCC})	%	40.4	40.4
HCS energy efficiency (η_{HCS})	%	14.7	14.7
HCS exergy efficiency (ψ_{HCS})	%	36.1	36.1
Integrated system energy efficiency (η_{ov})	%	16.8	24.8
Integrated system exergy efficiency (ψ_{ov})	%	27.8	40.9
Hydrogen production rate	kg/s	6.28	9.12
Hydrogen consumed for SCC	kg/s	2.72	3.88
Net hydrogen produced at high pressure (700 bar)	kg/s	3.56	5.24

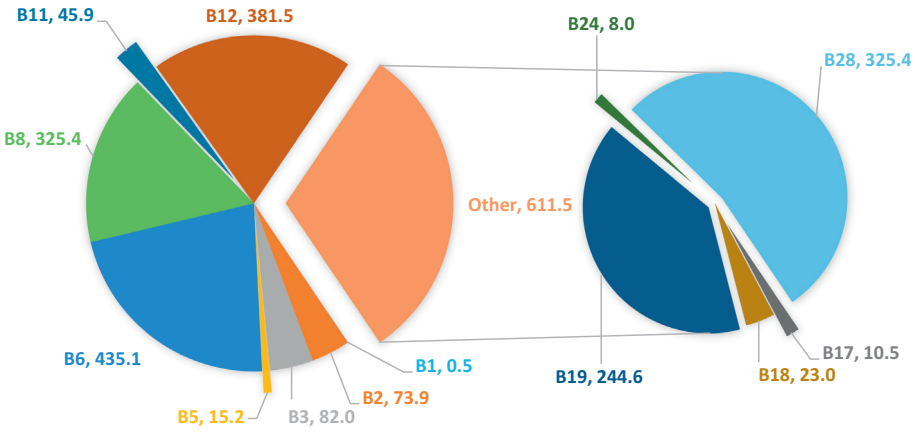

Fig. 6a. Thermal energy interactions in the Cu-Cl cycle reactors per mole of hydrogen produced in the cycle (kJ/mol H_2) (see Fig. 2a for reactor locations).

The overall energy and exergy efficiencies respectively of the overall integrated system are

$$\eta_{ov} = \frac{\dot{m}_{H_2}^{HP}(LHV_{H_2} + (h_{T\&P} - h_{T_o\&P_o}))}{\dot{Q}_{SCWR}} \quad (13)$$

$$\psi_{ov} = \frac{\dot{m}_{H_2}^{HP}(ex_{H_2})}{\dot{E}x_{\dot{Q}_{SCWR}}} \quad (14)$$

4. Results and discussion

The results of the simulation and thermodynamic analysis of the proposed integrated system are reported in Table 4, which lists the energy and exergy efficiencies of the proposed integrated system plus the hydrogen production rate for the two cases considered. The heat interactions and the associated exergy for each reactor in the Cu-Cl cycle (see Fig. 2a for reactor names) are shown in Fig. 6. The Cu-Cl cycle reactor that requires most of the cycle heat per mole of hydrogen produced is the Cu_2OCl_2 decomposition reactor (B6 in Fig. 2a). The Cu_2OCl_2 decomposition reactor also has the highest exergy consumption in the Cu-Cl cycle. The reactor that produces the most of the heat per mole of hydrogen produced within the cycle is the CuCl solidification reactor (B8 and B28 in Fig. 2a). There are four components in the system that release thermal energy, part of which is absorbed by the circulating steam in the steam circuit while the remainder is rejected to the environment. The four components are B8, B11, B24, and B28 (see

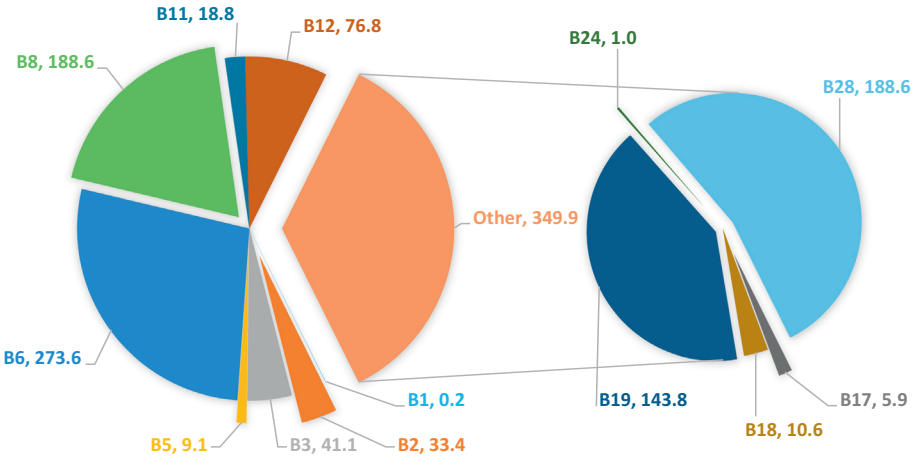

Fig. 6b. Thermal exergy interactions in the Cu-Cl cycle reactors per mole of hydrogen produced in the cycle (kJ/mol H_2) (see Fig. 2a for reactor locations).

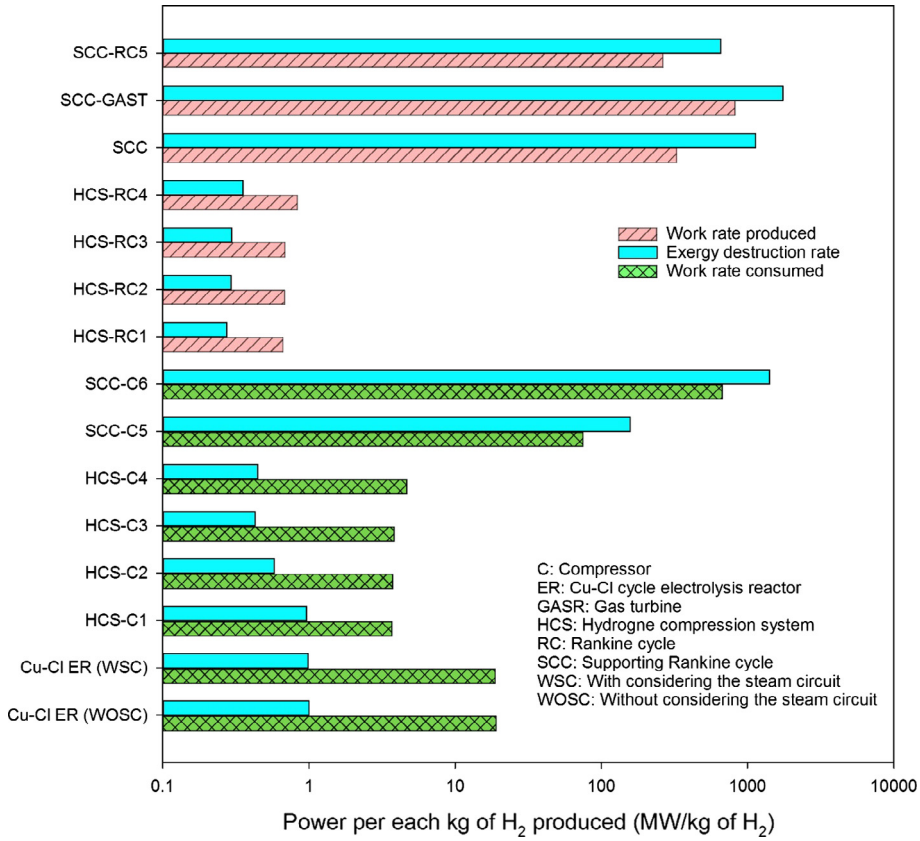

Fig. 7. Work rates and exergy destruction rates per kg of hydrogen produced by the integrated system for work rate producing and consuming devices.

Fig. 2a), where blocks B8 and B28 are the phase change reactors for solidifying the CuCl, and blocks B11 and B24 are ambient temperature coolers which cool the solid CuCl to a temperature lower than 90 °C so that it can enter the electrolysis reactor. Most of the thermal energy is released by the liquid CuCl during its solidification while the sensible heat released by the solidified CuCl is much less. That is why the CuCl solidification reactors release most of the thermal energy in the Cu-Cl cycle.

The work rates per kilogram of hydrogen produced for work rate consuming and producing devices in the integrated system are shown in Fig. 7. The component with the highest work production rate is the gas turbine (GAST in Fig. 5) in the SCC system then followed by the steam turbine in the SCC system, which both provide the power required by the compression system and by the Cu-Cl cycle electrolysis reactor. Having the SCC system producing most of the work in the system is expected since the SCC system is designed to fulfil all power requirements of the integrated system. The component with the highest work consumption rate per unit hydrogen produced is the hydrogen compressor (C6 in Fig. 5) in the SCC system. The work producing or consuming device with the highest exergy destruction rate per kg of hydrogen produced is the SCC gas turbine (GAST). This is reasonable since the SCC gas turbine is responsible for the production of high work rates per kg of hydrogen produced. The high work consumption by the hydrogen compressor is also observed in the energy and exergy efficiencies of the SCC system, which show that the two compressors plus the pump in the bottoming Rankine cycle of the SCC consume nearly 60% of the total power produced by the SCC system.

The energy and exergy efficiencies of the Cu-Cl cycle without considering the steam circuit are close to those reported in the literature. Without considering the steam circuit means without considering the method of delivering the heat to the cycle, and instead considering the heat required by the reaction and other heating or cooling processes. The energy and exergy efficiencies for non-steam circuit Cu-Cl cycle are found here to be 38.2% and 69.2% respectively. These values are very close to the corresponding efficiencies of 44.8% and 73.0% respectively reported by Orhan, Dincer and Rosen [11–13]. There are several reasons for the differences. First, in the current design the hydrogen produced is allowed to cool without recovering the heat for safety purposes. The extra steam provided to the hydrolysis reactor to obtain 100% conversion of the reactants is considered in this model, but not by Orhan, Dincer and Rosen [11–13]. Since the Cu-Cl cycle is integrated with a nuclear reactor producing heat in the form of supercritical superheated steam, the steam circuit which provides and recovers heat for the cycle needs to be considered.

The HCS bottoming Rankine cycles are found to reduce the required compression power by 18%. The remaining 82% is covered by the SCC. Most (90%) of the power produced by the SCC cycle is used for the electrolysis reactor in the Cu-Cl cycle and the remaining 10% drives the HCS compressors. As shown in Fig. 8, the energy efficiency of the HCS is 14.7%. This low value is due to the high work rate that is provided to the system to increase the pressure of the hydrogen while maintaining a final temperature of the compressed hydrogen as low as possible. The exergy efficiency of the HCS is 36.1%, which is higher than its energy efficiency because in the exergy analysis the high pressure compressed gas has a high exergy content. Also shown in Fig. 8 are the energy and exergy efficiencies of the SCC, which are 39.7% and 40.4% respectively.

In the first case, a specific steam circuit design is proposed, which is presented in Figs. 1 and 3. The proposed steam circuit design uses more heat from the nuclear reactor per kg of hydrogen produced than what the Cu-Cl cycle actually needs. The extra heat from the nuclear reactor is accounted for by the heat losses in the circuit. These cause the energy efficiency of the Cu-Cl cycle to be lower than the efficiency of the Cu-Cl cycle without considering the heat delivery method. The second case considers only the heat that is required by the Cu-Cl cycle to produce the hydrogen. The energy and exergy efficiencies of the main components of the integrated system for the first and the second cases are shown in Fig. 8. The exergy destruction ratio of the main components of the integrated system for the two cases considered are shown in Fig. 9. The energy efficiency of the Cu-Cl cycle (see Table 4) decreases from 38.2% to 27.2% and the exergy efficiency decreases from 69.2% to 50.7% when the proposed steam circuit design is considered. The drop in efficiencies of the Cu-Cl cycle indicates the importance of considering the steam circuit in the analysis of the Cu-Cl cycle when the heat provided to the cycle is from steam. Considering the steam circuit is also important due to its effect on the overall efficiencies and the hydrogen production rate. The overall energy efficiency of the hydrogen plant decreases from 24.8% to 16.8% and the exergy efficiency decreases from 40.9% to

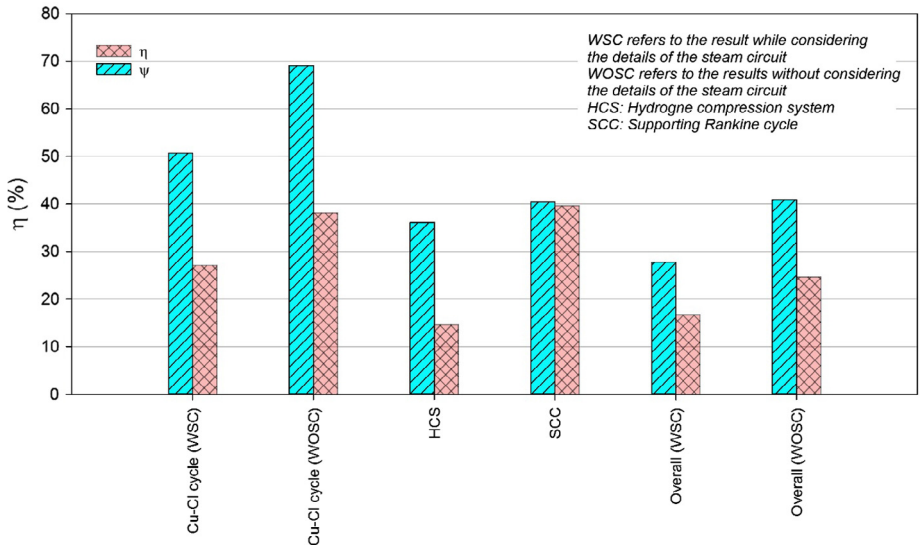

Fig. 8. Energy and exergy efficiencies of the main subsystems of the integrated system for two cases: the WSC case in which the steam circuit is considered in the analysis of the integrated system and the WOSC case in which the steam circuit is not considered in the analysis of the integrated system.

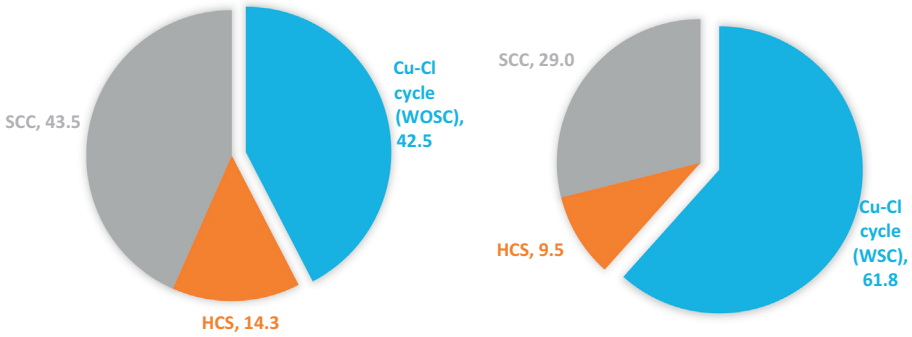

Fig. 9. Exergy destruction breakdowns (%) for two cases: on the right the case where the steam circuit is considered in the analysis, and on the left the case where the steam circuit is not considered.

27.8% when the steam circuit design is considered. The hydrogen production rate decreases from 5.24 kg/s to 3.56 kg/s when the SC is considered in the analysis (see Table 4). Note that the hydrogen is produced at a pressure of 700 bar. The exergy destruction contributions of the main components in the overall cycle are shown in Fig. 9. The contribution of the Cu-Cl cycle to the overall exergy destruction rate of the integrated system increases when the steam circuit is considered. This is in part because of the corresponding increase in the mass flow rate of hydrogen to the SCC. The mass ratio of the hydrogen conveyed to the SCC increases from 42.5% to 43.3% when the steam circuit is considered in the analysis.

5. Conclusions

An integrated system which mainly consists of the supercritical water-cooled nuclear reactor, a hybrid thermochemical water decomposition cycle (utilizing a copper-chlorine cycle), a combined cycle, and a hydrogen compression system is proposed and investigated comprehensively. In this integrated system, a novel design is considered of the hybrid thermochemical water decomposition cycle with all subprocesses. The steam provides the cycle with its required heat and is used in heat recovery from some components in the cycle. The effects of the steam circuit on the performance of the hybrid thermochemical cycle and the overall system are examined. The effect of the steam circuit on the performance is found to be significant. The results indicate that:

- The hydrogen production rate is 3.56 kg/s, and it is delivered at a high pressure (700 bar).
- When the steam circuit is considered, the energy efficiency of the proposed integrated system is found to be 16.8% and the exergy efficiency 27.8%.
- The energy and exergy efficiencies of the hydrogen compression system are 14.7% and 36.1%, respectively.
- The energy and exergy efficiencies of the supporting Rankine cycle are 39.7% and 40.4%, respectively.

The present results suggest, in efforts at integrating the hybrid thermochemical water decomposition cycle utilizing the chemical couple copper and chlorine, the method of delivering heat to or recovering heat from the cycle needs to be carefully considered.

Acknowledgement

The authors acknowledge the support provided by the Natural Sciences and Engineering Research Council of Canada.

References

[1] Dincer I, Zamfirescu C. Sustainable hydrogen production. Elsevier; 2016.
[2] Naterer GF, Dincer I, Zamfirescu C. Hydrogen as a clean energy carrier. In: Hydrogen production from nuclear energy. Springer; 2013. p. 1–20.
[3] Naterer GF, Dincer I, Zamfirescu C. Water electrolysis. In: Hydrogen production from nuclear energy. Springer; 2013. p. 99–152.
[4] Naterer GF, Dincer I, Zamfirescu C. Thermochemical water-splitting cycles. In: Hydrogen production from nuclear energy. Springer; 2013. p. 153–272.
[5] Administration USEI. April 2016. Monthly energy review. U.S. energy information administration; 2016.
[6] Al-Zareer M, Dincer I, Rosen MA. Effects of various gasification parameters and operating conditions on syngas and hydrogen production. Chem Eng Res Des 2016;115:1–18.
[7] Abuadala A, Dincer I, Naterer GF. Exergy analysis of hydrogen production from biomass gasification. Int J Hydrogen Energy 2010;35:4981–90.
[8] Dincer I, Joshi AS. Solar hydrogen production. In: Solar based hydrogen production systems; 2013. p. 27–71.
[9] Hewitt GF, Collier JG. Introduction to nuclear power. Taylor & Francis; 2000.
[10] Duffey RB, Pioro IL. Supercritical water-cooled nuclear reactors: review and status. Nuclear energy materials and reactors. In: Nuclear materials and reactors from encyclopedia of life support systems (EOLSS), developed under the auspices of the UNESCO. Oxford: EOLSS Publishers; 2005.
[11] Orhan MF, Dincer I, Rosen MA. Efficiency analysis of a hybrid copper-chlorine (Cu-Cl) cycle for nuclear-based hydrogen production. Chem Eng J 2009;155:132–7.
[12] Orhan MF. Conceptual design, analysis and optimization of nuclear-based hydrogen production via copper-chlorine thermochemical cycles. Doctoral dissertation, Faculty of Engineering and Applied Science, Mechanical Engineering Program. University of Ontario Institute of Technology, Oshawa, Canada, April 2011.
[13] Orhan MF, Dincer I, Rosen MA. Efficiency comparison of various design schemes for copper–chlorine (Cu–Cl) hydrogen production processes using Aspen Plus software. Energy Convers Manage 2012;63:70–86.
[14] Ratlamwala TAH, Dincer I. Energy and exergy analyses of a Cu–Cl cycle based integrated system for hydrogen production. Chem Eng Sci 2012;84:564–73.
[15] Al-Zareer M, Dincer I, Rosen MA. Development and analysis of an integrated system with direct splitting of hydrogen sulfide for hydrogen production. Int J Hydrogen Energy 2016;41:20036–62.
[16] Ozbilen A, Dincer I, Rosen MA. Development of new heat exchanger network designs for a four-step Cu-Cl cycle for hydrogen production. Energy 2014;77:338–51.
[17] Naterer GF, Dincer I, Zamfirescu C. Nuclear energy and its role in hydrogen production. In: Hydrogen production from nuclear energy. Springer; 2013. p. 21–64.
[18] Dincer I, Rosen MA. Exergy: energy, environment and sustainable development. 2nd ed. Elsevier; 2012.
[19] Bushby SJ, Dimmick GR, Duffey RB, Spinks NJ, Burrill KA, Chan PSW. Conceptual designs for advanced, high-temperature CANDU reactors. In: Proceedings of the 1st international symposium on supercritical water-cooled reactor design and technology (SCR-2000), Tokyo, Japan, November 6–8, Paper 103.
[20] Boggs BK, Botte GG. On-board hydrogen storage and production: an application of ammonia electrolysis. J Power Sources 2009;192:573–81.
[21] Toyota Canada: Toyota to Increase "Mirai" Production; 2014. http://www.toyota.ca/toyota/en/company-info/news/post/toyota-to-increase-mirai-production [accessed September 13, 2016].
[22] Nguyen-Schäfer H. Rotordynamics of automotive turbochargers. Springer; 2012.
[23] Zamfirescu C, Dincer I, Naterer GF. Thermophysical properties of copper compounds in copper-chlorine thermochemical water splitting cycles. Int J Hydrogen Energy 2010;35:4839–52.

[24] Parry T. Thermodynamics and magnetism of Cu2OCl2. Masters dissertation, Department of chemistry and biochemistry. Brigham Young University, Provo, Utah, December 2008.
[25] Chase Jr MW. NIST-JANAF thermochemical tables. In: Journal of physics and chemistry reference data, 4th ed., Monograph 9; 1998.
[26] Perry RH, Green DW, Maloney JO. Perry's chemical engineers' handbook. McGraw-Hill; 1984.
[27] Lide DR. CRC handbook of chemistry and physics: a ready-reference book of chemical and physical data. CRC Press; 2008.
[28] Knacke O, Kubaschewski O, Hesselmann K. Thermochemical properties of inorganic substances. Springer-Verlag; 1991.